THE ASTROPHYSICAL JOURNAL, 407:519–524, 1993 April 20

THE CONTINUUM SLOPES AND EVOLUTION OF ACTIVE GALACTIC NUCLEI[1]

PAUL J. FRANCIS
Steward Observatory, University of Arizona, Tucson, AZ 85721
Received 1992 June 16; accepted 1992 October 19

ABSTRACT

Studies of the evolution of active galactic nuclei (AGNs) have mostly used a single continuum slope to compute *k*-corrections. In this paper it is shown that allowing for the observed diversity of AGN continuum shapes greatly affects measurements of both the continuum slopes and number evolution. Less evolution is required between redshift two and the present, and a spurious correlation between continuum slope and redshift introduced in magnitude-limited samples.

Two reported correlations between continuum slope and redshift are shown to be consistent with this spurious origin. However, observations of QSOs from the Large Bright QSO Survey show that luminous high-redshift QSOs have intrinsically harder optical-UV continuum slopes. It is concluded that this is an evolutionary effect and not a correlation with luminosity.

Subject heading: quasars: general

1. INTRODUCTION

It is now well established that there is a considerable diversity in the continuum energy distributions of quasi-stellar objects (QSOs) in every observed waveband (e.g., McDowell et al. 1989; Ward et al. 1987; Williams et al. 1992). Many physical mechanisms contribute to this diversity, and much of it may not be intrinsic to the active galactic nuclei (AGNs) (Cheng, Gaskell, & Koratkar 1991). However, regardless of the origin of this diversity, it will have substantial effects on QSO number counts in magnitude-limited samples (Hewett 1992; Giallongo & Vagnetti 1992). For example, the *k*-corrections calculated for $z = 3$ QSOs using power-law continuum slopes with indices differing by 1 (well within the observed range both in the optical [Francis et al. 1991] and X-ray [Wilkes & Elvis 1987]) will differ by more than 1.5 mag, which, given the steepness of QSO luminosity functions (Boyle, Shanks, & Peterson 1988), can correspond to a factor of over 200 in observed number density.

The range of continuum energy distributions has been allowed for in the computation of radio source evolution: Peacock (1985) showed that by separating radio sources into the two classes of steep and flat spectrum QSOs and by using different *k*-corrections, a satisfactory picture of their evolution could be obtained. In the optical and X-ray, however, the use of a single mean continuum slope to compute *k*-corrections has been nearly universal.

In this paper the effects of this continuum slope diversity upon QSO number counts are investigated. In § 2 a simple model for QSO populations observed at different rest-frame wavelengths is developed. The model predictions are compared with observed continuum slopes in § 3, and the consequences for quasar evolution are discussed in § 4. The results are summarized in § 5.

A note on nomenclature: rather than use such potentially ambiguous terms as "flat" or "steep" spectra, I will use the terms "hard" and "soft" to describe continuum slopes at all wavelengths. Continuum slopes are parameterized by a power law: I use the convention that the flux per unit frequency f_ν is proportional to the frequency ν raised to the power α, that is, that $f_\nu \propto \nu^\alpha$. Thus a "hard" spectrum is one with a more positive value of α.

2. THE MODEL

Consider a population of QSOs observed at a particular rest-frame wavelength. If the same population is studied using a magnitude-limited sample selected at a shorter rest-frame wavelength, the QSOs with hard spectra will appear brighter than those with average or soft spectra and hence will predominate in the new sample. Thus both the mean continuum slope and the number counts of QSOs can be affected by the dispersion in continuum slopes.

Giallongo & Vagnetti (1992) include the effects of a dispersion in the continuum slopes by treating it as a redshift-dependent magnitude uncertainty. In this paper a different approach is taken—the distribution of QSOs in both luminosity and continuum slope is modeled as a function of the selection wavelength. This latter approach shows that the continuum slopes measured will be a strong function of the selection wavelength. These mean continuum slopes in turn have a strong effect upon *k*-corrections and hence on measurements of QSO evolution.

2.1. *Calculations*

Any population of AGNs can be described by a distribution function $n(L_0, \alpha)$, where n is the number of AGNs per unit luminosity L_0, (measured at some rest-frame wavelength λ_0) and per unit continuum slope α. In this section the distribution $n(L_1, \alpha)$ of the same sample, but with the luminosity measured at some different rest-frame wavelength λ_1, is calculated, assuming a particular functional form for $n(L_0, \alpha)$. This calculation applies both to samples at the same redshift selected in different passbands, and to samples at different redshifts selected in the same observed passband.

Let us assume a particular distribution function $n(L_0, \alpha)$ for an AGN sample with luminosities L_0 measured at rest-frame wavelength λ_0. The first assumption is that the distribution of continuum slopes is independent of the luminosity, that is, that

[1] Observations reported here were obtained with the Multiple Mirror Telescope, a facility operated jointly by the Smithsonian Institution and the University of Arizona, and with the Las Campanas Observatory, a facility of the Carnegie Institution of Washington.

$n(L_0, \alpha)$ can be rewritten as $n_1(L_0)n_2(\alpha)$. The purpose of this calculation is to demonstrate the effects of a dispersion in continuum slopes, and so this additional complication has been neglected, although as will be shown in § 3.2 intrinsic continuum slopes may well be a function of luminosity or redshift. A power-law luminosity function will be used [$n_1(L_0) \propto L_0^{\beta}$], which as shown by Boyle et al. (1988) and Della Ceca et al. (1992) is a reasonable approximation for restricted luminosity ranges both in the optical and X-ray. Depending on the waveband employed and the AGN luminosities, $-1.5 \gtrsim \beta \gtrsim -3.9$ (Boyle 1992).

The continuum is modeled as a power law ($F_\nu \propto \nu^\alpha$), which is an approximation valid only for restricted wavelength ranges (e.g., Francis et al. 1991). The distribution of power-law indices α is taken to be a Gaussian, both for simplicity's sake and as suggested by optical observations (Francis et al. 1991, 1992). The power-law index has a mean α_0 and a standard deviation σ, both measured from a sample selected at wavelength λ_0. The effects of different assumptions will be discussed below.

The distribution function is thus

$$n(L_0, \alpha) \propto L_0^{\beta} e^{-(1/2)[(\alpha-\alpha_0)/\sigma]^2} . \quad (1)$$

The luminosity L_1 at some other wavelength λ_1 is given by

$$\frac{L_1}{L_0} = \left(\frac{\lambda_1}{\lambda_0}\right)^{-(\alpha+1)} \quad (2)$$

on the assumption that the rest-frame width of the passband employed in measuring the luminosity is proportional to its wavelength. This will be the case for AGNs at different redshifts being measured in the same rest-frame passband, but if different passbands are used, the equation must be scaled by a constant multiplier to allow for the relative widths of the different passbands. Line radiation will not affect the results derived here by more than a constant, unless the line fluxes correlate strongly with the continuum slope, which is not the case in the rest-frame UV (Francis et al. 1992).

Writing $\lambda_1/\lambda_0 = r$, and changing variables, we find that

$$n(L_1, \alpha) \propto L_1^{\beta} r^{(\alpha+1)(\beta+1)} e^{-(1/2)[(\alpha-\alpha_0)/\sigma]^2} , \quad (3)$$

and, after completing the square in the exponent,

$$n(L_1, \alpha) \propto L_1^{\beta} r^{(\alpha_0+1)(\beta+1)} e^{-(1/2)\{\alpha-[\alpha_0+\sigma^2(1+\beta)\log_e(r)]\}^2/\sigma^2} \times e^{(\sigma^2/2)[(1+\beta)\log_e(r)]^2} . \quad (4)$$

The form of this distribution is similar to the original distribution (eq. [1]); there is a power-law dependence upon the luminosity with the same index β, and a Gaussian distribution of power-law indices α with the same standard deviation σ. The standard k-correction term ($r^{(\alpha_0+1)(\beta+1)}$) appears, as would be needed if all QSOs had identical continuum slopes of α_0. There are, however, two new features introduced by the dispersion in the continuum slopes. Firstly, the mean value of α has increased by $\sigma^2(1+\beta)\log_e(r)$. As $\beta < -1$, this means that at shorter wavelengths, a harder mean slope will be measured. Second, the last term increases the measured numbers of QSOs above the amounts predicted by the simple k-corrections for r different from 1. This can be understood as follows: when a sample of QSOs selected at λ_0 is studied, equal numbers are found with hard spectra ($\alpha > \alpha_0$) and with soft spectra ($\alpha < \alpha_0$). For a QSO sample magnitude limited at the new wavelength λ_1, the numbers are no longer equal. However, as the luminosity function is nonlinear (a power law), the changes in the numbers of the two subpopulations do not balance. For example, if $\lambda_1 < \lambda_0$, the increase in the observed numbers of hard-spectrum QSOs will exceed the drop in the numbers of soft-spectrum QSOs.

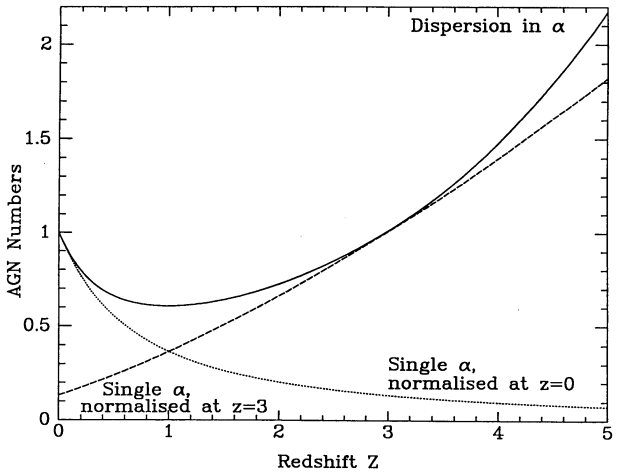

FIG. 1.—AGN numbers as a function of redshift, assuming no evolution in the AGN population and ignoring cosmological factors. The solid line includes the effect of a dispersion ($\sigma = 0.5$) in continuum slopes and has a mean continuum slope of -0.5 for a zero redshift sample. The dotted line gives the AGN numbers as a function of redshift if there is no dispersion in continuum slopes, with the same mean zero redshift slope of -0.5. The dashed line gives AGN numbers in the absence of a dispersion in continuum slopes, assuming a continuum slope equal to the mean that would be measured from the "with dispersion" sample at $z = 3$.

This result seems contradictory: how can the predicted number of QSOs rise above a power law both when extrapolating from λ_1 to λ_2, and when extrapolating from λ_2 to λ_1? The answer is illustrated in Figure 1. The solid line shows the predicted AGN numbers as a function of redshift, assuming that the mean continuum slope of a sample selected at zero redshift is -0.5, that $\beta = -3.9$ (Boyle et al. 1988), and that the standard deviation of the continuum slope distribution is 0.5 (Table 1). The dotted line shows the prediction using a single power law with $\alpha = -0.5$ to perform the k-corrections. As discussed, the inclusion of a dispersion in α raises the predicted numbers well above the single power-law prediction. If, however, rather than taking a zero redshift sample and extrapolating to large redshifts, we took a redshift three sample and extrapolated to smaller redshifts, we would measure a different (harder) mean continuum slope, and so the single power-law prediction is now the dashed line. Once again, the dispersion-included prediction lies above the single power-law prediction.

The message is that in addition to allowing for a dispersion in the continuum slopes, attention must be paid to the redshift of the QSOs from which the mean continuum slope is derived.

Thus, the predictions of this model are that the mean continuum slopes of QSOs should be harder when observed at shorter wavelengths, and that the numbers of QSOs predicted from a sample observed at a particular wavelength using a single power-law luminosity function in the k-corrections is an underestimate of what should actually be observed.

3. CONTINUUM SLOPES AS A FUNCTION OF REDSHIFT

A prediction of the above calculations is that correlations between continuum hardness and redshift should be seen in AGN samples, simply because of the effect of the dispersion of

slopes on the AGN numbers. In this section the detailed model predictions are compared with two literature studies, and with detailed optical observations of a large QSO survey.

3.1. *Existing Studies*

O'Brien, Gondhalekar, & Wilson (1988) identified a correlation between redshift and the hardness of the UV-optical spectra of AGNs in a collection of objects with *IUE* observations. While their sample is not in any sense complete, most of the individual AGNs in it come from samples with some optical magnitude limit, which is not a function of redshift, and hence the calculations in § 2 should apply. They measure $d\alpha/d \log (1 + z) = 0.79 \pm 0.20$. Equation (4) predicts that for $\sigma = 0.5$ (Francis et al. 1991) and $\beta = -3.9$ (Boyle et al. 1988), $d\alpha/d \log (1 + z) = 0.73$, in good agreement with the observed value. Thus no evolution of AGN UV-optical continuum slopes is required, only the tendency of high-redshift samples to be biased towards AGNs with harder continua.

Williams et al. (1992) report that the hardness of the X-ray spectra of a sample of high-luminosity AGNs observed by *GINGA* correlates with, among other things, luminosity. They do not give a fit to the relation, but visual inspection of the relevant figure gives $d\alpha/d \log (1 + z) \sim 0.3$. They also determine a standard deviation of continuum slopes in the 2–10 keV range of $\sigma = 0.31$. Combining this value of σ with a luminosity function with $\beta = -3.2$ (Boyle 1992), the predicted $d\alpha/d \log (1 + z) = 0.21$, not inconsistent with the measured value.

Thus two literature reports of continuum slope/redshift correlations are consistent with nothing more than the bias of high-redshift samples toward hard-spectrum AGNs.

3.2. *Observations*

In order to more stringently test the continuum slope/redshift correlation against the model, observations of the Large Bright QSO Survey (LBQS) have been used. The uniformity and size of the LBQS allows good statistics to be compiled and for the effect of variable k-corrections to be well accounted for.

The LBQS is described in Foltz et al. (1987, 1989), Hewett et al. (1991), Chaffee et al. (1991), and Morris et al. (1991). It consists of data on more than 1000 QSOs, with redshifts $0.2 \leq z < 3.4$, apparent magnitudes $16.0 \leq m_{B_J} \leq 18.85$, and absolute magnitudes $M_{B_J} \leq -21.5$ (for $q_0 = 0.5$, $H_0 = 100$ km s^{-1} Mpc^{-1}). While the quantification of the LBQS sensitivity to different QSO types is incomplete (Hewett 1993), comparisons with existing surveys suggest that the only class of QSOs missed will be BL Lac objects, due to their lack of emission lines and their extremely red ($\alpha < -2$) continuum slopes.

As the large-scale UV-optical continuum shape of QSOs is not a power law (Francis et al. 1991), continuum slope measurements must be made at constant rest-frame wavelengths to avoid trends with redshift due only to the large-scale continuum shape. Three pairs of continuum windows were used, 1430–1480 to 2150–2230 Å, 2150–2230 to 3020–3100 Å, and 3020–3100 to 4150–4250 Å. Each continuum window was chosen to avoid strong emission lines. Using the mean flux in each continuum window, power laws were fitted to each spectrum with such a redshift that both of a given pair of continuum windows appeared in the observed-frame wavelength range 3750–6400 Å. This observed-frame wavelength range was chosen to ensure that light losses due to differential atmospheric refraction, and second-order light in the spectrograph, did not alter the measured continuum slopes. Poisson noise in the spectra introduces an uncertainty of ~ 0.02 in the power-law indices.

3.3. *Results*

The measured continuum slopes for the three pairs of continuum windows are shown in Figure 2, as a function of redshift. As predicted, continuum hardness correlates with redshift for every pair of continuum windows. All three correlations were tested for significance using the Spearman's Rank Correlation Coefficient (RS): the results are shown in Table 1. The two-tailed probabilities (Prob) of such a correlation being the result of chance are less than 2% for the reddest pair of windows, and even less likely for the other window pairs.

The size of the redshift/continuum-slope correlation was measured by performing linear least-squares fits to the α/z relations in Figure 2. The results are shown in Table 1 and compared with the calculated correlation slope, using equation (4), and the measured σ-values. Errors are dominated by the intrinsic scatter in α, not the limited signal-to-noise ratio of individual spectra. In all cases, the observed slope of the correlation is

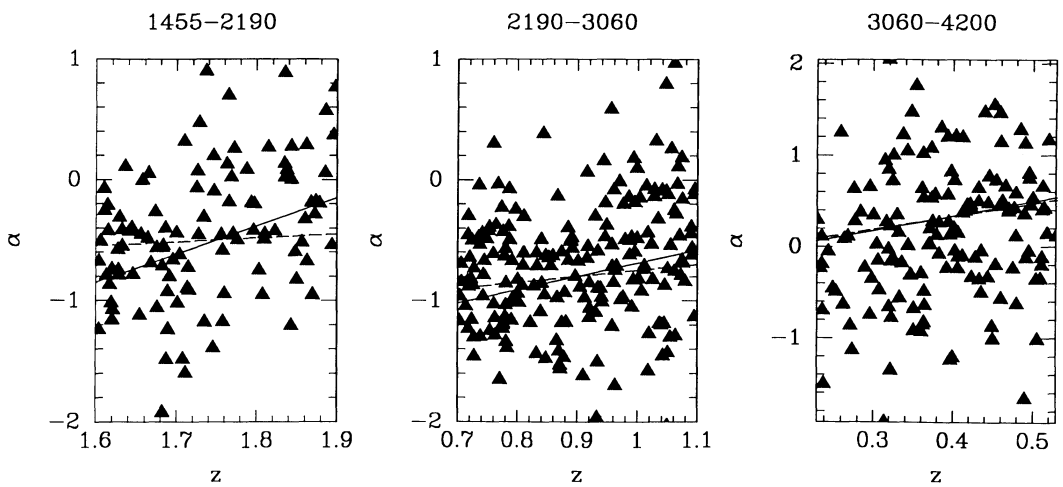

FIG. 2.—Continuum power-law indices α ($F_\nu \propto \nu^\alpha$) as a function of redshift z for three different pairs of rest-frame continuum windows, 1455–2190, 2190–3060, and 3060–4200 Å. Solid lines are least-squares fits to the data, and dashed lines are model predictions assuming no intrinsic correlation between continuum slope and redshift.

TABLE 1

CONTINUUM SLOPE/REDSHIFT CORRELATIONS

Continuum Wavelengths (Å)	Number of QSOs	Mean α	σ	Measured $d\alpha/dz$	RS	Prob	Model $d\alpha/dz$
1455–2190	105	−0.5	0.5	2.3 ± 0.6	0.29	0.002	0.36
2190–3060	200	−0.8	0.5	1.1 ± 0.3	0.25	0.0003	0.53
3060–4200	145	+0.3	0.7	1.6 ± 0.7	0.20	0.016	1.4

greater than the predicted one, and for the 1455–2190 Å measurements, the discrepancy is significant at the 3 σ level.

Could this trend be due to dust in our own Galaxy? Higher redshift QSOs will be observed at longer observed-frame wavelengths and hence will be less reddened. Given the high Galactic latitude ($> 50°$) of the LBQS QSOs, however, and using the dust extinction law of Savage & Mathis (1979), this effect should only introduce a $d\alpha/dz < 0.1$, which is insufficient to affect the result.

To test the reality and nature of this excess intrinsic correlation, new subsamples of QSOs were constructed, magnitude limited not in an observed-frame passband, but at a constant rest-frame wavelength. Using the B_J magnitudes to calibrate the spectra, the fluxes and flux limits in one of the continuum windows were calculated. All QSOs with fluxes below the largest flux limit were excluded. The resultant samples should be free from the redshift/continuum-slope correlations calculated in § 2; only intrinsic effects should remain. Monochromatic luminosities were computed from the fluxes in the continuum window used to limit the sample, using $q_0 = 0.5$. The luminosities of each subsample were divided by the sample mean—that is, normalized to a mean of one.

The redshifts and luminosities of the LBQS QSOs are correlated, making the interpretation of any observed correlations complex. To allow for this, the correlation of continuum slope with luminosity and redshift were calculated separately, holding the other constant. This was done as follows: a least-squares fit was made of luminosity against redshift, and vice versa. This allowed a mean luminosity for any given redshift, and a mean redshift for any given luminosity, to be computed. For each QSO, the mean redshift of QSOs with that luminosity was subtracted from its individual redshift, resulting in a normalized redshift. Similarly, each luminosity had the mean luminosity of a QSO with that redshift subtracted from it. The resultant normalized redshifts and luminosities are independent, and so the correlations of each separately with continuum slope can be investigated.

The results are shown in Figure 3 and Table 2. Little can be said for the 1455–2190 Å pair of continuum windows due to the limited number of QSOs meeting the rest-frame magnitude limits. In both the remaining pairs of continuum regions, the correlation between continuum slope and redshift is confirmed at a high level of significance (Table 2). The Spearman's Rank Correlation Coefficient (RS) has been computed, and the two-tailed probabilities that the observed correlation is due to chance are less than 0.5%. The 3060–4200 Å region has one QSO much more luminous than the rest, and the calculation was repeated without this object as a check: as shown in Table 2 this does not significantly alter the results. The slopes of the relationships have been computed by least-squares fitting: the errors are dominated by the intrinsic scatter in continuum slopes, and not by observational errors.

The correlations of continuum slope with luminosity are much weaker. In no case are they significant at the 90% level. Indeed, for the 2190–3060 Å continuum wavelength pair, more

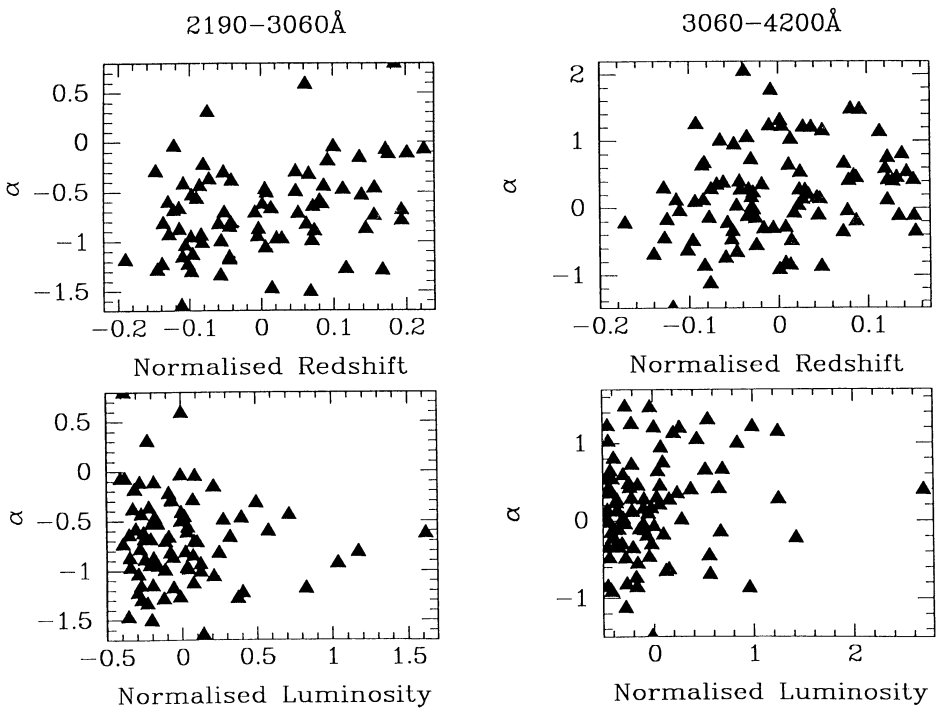

FIG. 3.—Continuum power-law indices α ($F_\nu \propto \nu^\alpha$) as a function of both redshift z, and continuum luminosity. QSO samples magnitude limited at a constant rest-frame wavelength have been used. Both redshifts and luminosities have been normalized as described in the text to make them mutually independent.

TABLE 2

REST-FRAME LIMITED SAMPLE CORRELATIONS

CONTINUUM WAVELENGTHS (Å)	NUMBER OF QSOs	z CORRELATION			L CORRELATION		
		$\partial\alpha/\partial z$	RS	Prob	$\partial\alpha/\partial L$	RS	Prob
2190–3060	80	1.34 ± 0.4	0.32	0.004	-0.11 ± 0.13	−0.07	0.55
3060–4200[a]	92	2.21 ± 0.8	0.29	0.005	0.18 ± 0.13	0.15	0.16
3060–4200[b]	91	2.18 ± 0.8	0.28	0.006	0.25 ± 0.15	0.16	0.13

[a] Including all objects.
[b] Excluding one extreme object.

luminous QSOs actually have marginally softer spectra. This result is independent of the value of q_0 used to compute luminosities. *This result suggests that the correlation is an evolutionary one.* This is in agreement with the results of Sargent, Steidel, & Boksenberg (1989) and Tytler & Fan (1992) who find either no correlation between AGN luminosity and continuum slope, or that more luminous AGNs have softer UV-optical continuum slopes.

All the continuum windows employed will contain some flux from blended line emission, in particular from Fe II (Wills, Netzer, & Wills 1985). It is possible that the strength of this emission might correlate with luminosity or redshift and produce the observed correlations; however, it is unlikely that such line emission would introduce a correlation in the same sense between all the pairs of continuum windows. A second possible contaminant is light from the QSO's host galaxy. The absolute magnitude cutoff of the LBQS was chosen to minimize this, and at most it should only affect the longest wavelength pair of continuum windows.

Note also that the mean slope in the reddest pair of continuum windows is substantially harder than the mean in the other two. This is a reflection of the nonpower-law nature of the UV-optical energy distributions of AGNs (e.g., Oke, Shields, & Korycansky 1984; Francis et al. 1991).

In conclusion, the observed correlation between the hardness of the continuum radiation and the redshift is larger than that predicted by the model in § 2. An additional intrinsic correlation is required, and it appears to be a correlation with redshift and not luminosity.

4. EVOLUTION OF AGN NUMBERS

It was shown in § 2 that a single continuum slope model is inadequate for comparing samples selected at different rest-frame wavelengths. Equation (4) shows that including a range of continuum slopes introduces a correction factor, the size of which depends on the rest-frame wavelength ratio r, the standard deviation of the continuum slope distribution σ, and the slope of the luminosity function β, defined by $n(L) \propto L^{\beta}$.

For a sample of AGNs magnitude limited at a constant observed-frame wavelength, r is given by the redshift. It is shown in Table 1 that $\sigma \sim 0.5$ in the UV-optical wavelength region. A value of $\sigma \sim 0.3$ is appropriate for 2–10 keV X-rays (Williams et al. 1992). The luminosity function of AGNs at all wavebands can be well represented by two power laws: a steep one ($\beta \sim -3.5$) for luminous AGNs and a flatter one ($\beta \sim -1.6$) for faint AGNs (Boyle 1992). The luminosity of the break in the power law strongly evolves with redshift. Given these numbers, the size of the corrections can be computed.

As an example, consider a sample observed at low redshift, with a mean power-law index of α_0 (Fig. 1). If an identical sample was observed at redshift 2, the observed number densities (solid line) will differ from those predicted using single-slope k-corrections (dotted line). For luminous AGNs observed in the rest-frame optical ($\beta = -3.9$) the correction factor is 3.5, that is, more than 3 times as many AGNs will be seen at redshift two than would be predicted if the range of continuum slopes was ignored. For less luminous optically selected AGNs, however ($\beta = -1.6$), the correction factor is only 1.05. The knee in the luminosity function thus moves predominantly in the direction of increased luminosity, so the correction factor has an effect upon the luminosity function similar to pure luminosity evolution.

In this case, allowing for the correction factor diminishes the evolutionary decline in AGN numbers inferred between redshift two and the present by a factor of 3.5. The sense of the correction does however depend upon the power-law index assumed in the calculation of the k-corrections. If this index was measured from high-redshift AGNs (dashed line in Fig. 1), the correction would go in the opposite sense, and more luminosity evolution would be required to explain the observed number counts than a single power-single index model would predict.

This example, with the mean continuum slope derived from measurements of $z = 0$ AGNs, is equivalent to the calculations of Giallongo & Vagnetti (1992) and gives the same result—less evolution between $z = 2$ and the present. However, Giallongo & Vagnetti use a mean continuum slope of $\alpha = -0.5$, which while close to that measured for high-redshift samples in the UV-optical (e.g., Table 1) is much softer than the continuum slopes measured from the lowest redshift LBQS QSOs ($\alpha = +0.3$, Table 1). Using the LBQS mean low-redshift AGN continuum slope increases k-corrections for $z = 2$ AGNs by ~ 0.8 mag, reducing the inferred AGN evolution by an even larger factor. This change is, however, partially undone by the softening of intrinsic continuum slopes at shorter rest-frame wavelengths.

In conclusion, the range of continuum slopes has a large effect upon the inferred evolution of the AGN population. As a caution, it should however be noticed that this discussion has neglected the evolution of AGN continuum slopes identified in § 3. This correlation between continuum slope and redshift not only complicates k-corrections, but also casts doubt upon the whole concept of correcting fluxes to a particular rest-frame wavelength, as different wavelengths will yield different amounts of evolution.

5. SUMMARY

1. The observed range of AGN continuum slopes needs to be taken into account when studying either the number counts or continuum slopes of AGNs. High-redshift ($z = 2$) optically

selected AGN samples will have harder mean continuum slopes ($\Delta\alpha \sim 0.8$) and have ~ 3.5 times more AGNs than would be predicted by extrapolating the properties of low-redshift ($z \sim 0$) samples using a single continuum slope. Allowing for a realistic range of continuum slopes will in general decrease the required evolution in the AGN population between redshift two and the present, but the exact change depends crucially upon how the continuum slopes used to perform the k-corrections are measured.

2. High-redshift AGNs have intrinsically harder UV-optical continuum slopes than low redshift AGNs. This appears to be a correlation with redshift and not with absolute magnitude.

I thank Paul Hewett, Craig Foltz, and Fred Chaffee for many helpful discussions. This work was partially supported by the National Science Foundation under grant AST 90-01181, for which we are grateful. I am supported by a SERC/NATO postdoctoral fellowship.

REFERENCES

Boyle, B. J. 1992, in Proc. Cambridge Conf. on Nature of Compact Object in AGN (Cambridge: Cambridge Univ. Press), in press
Boyle, B. J., Shanks, T., & Peterson, B. A. 1988, MNRAS, 235, 935
Chaffee, F. H., Foltz, C. B., Hewett, P. C., Francis, P. J., Weymann, R. J., Morris, S. L., Anderson, S. F., & MacAlpine, G. M. 1991, AJ, 102, 461
Cheng, F. H., Gaskell, C. M., & Koratkar, A. P. 1991, ApJ, 370, 487
Della Ceca, R., Maccacaro, T., Gioia, I. M., Wolter, A., & Stocke, J. T. 1992, ApJ, 389, 491
Foltz, C. B., Chaffee, F. H., Hewett, P. C., MacAlpine, G. M., Turnshek, D. A., Weymann, R. J., & Anderson, S. F. 1987, AJ, 94, 1423
Foltz, C. B., Chaffee, F. H., Hewett, P. C., Weymann, R. J., Anderson, S. F., & MacAlpine, G. M. 1989, AJ, 98, 1959
Francis, P. J., Hewett, P. C., Foltz, C. B., & Chaffee, F. H. 1992, ApJ, 398, 476
Francis, P. J., Hewett, P. C., Foltz, C. B., Chaffee, F. H., Weymann, R. J., & Morris, S. L. 1991, ApJ, 373, 465
Giallongo, E., & Vagnetti, F. 1992, ApJ, 396, 411
Hewett, P. C. 1992, in Proc. Heidelberg Conference on Physics of AGN, W. J. Dusch & S. Wagner (Berlin: Springer), 649
Hewett, P. C. 1993, in preparation
Hewett, P. C., Foltz, C. B., Chaffee, F. H., Francis, P. J., Weymann, R. J., Morris, S. L., Anderson, S. F., & MacAlpine, G. M. 1991, AJ, 101, 1121
McDowell, J. C., Elvis, M., Wilkes, B. J., Willner, S. P., Oey, M. S., Polomski, E., Bechtold, J., & Green, R. F. 1989, ApJ, 345, L13
Morris, S. L., Weymann, R. J., Anderson, S. F., Hewett, P. C., Foltz, C. B., Chaffee, F. H., Francis, P. J., & MacAlpine, G. M. 1991, AJ, 102, 1627
O'Brien, P. T., Gondhalekar, P. M., & Wilson, R. 1988, MNRAS, 233, 801
Oke, J. B., Shields, G. A., & Korycansky, D. G. 1984, ApJ, 277, 64
Peacock, J. A. 1985, MNRAS, 217, 601
Sargent, W. L., Steidel, C. C., & Boksenberg, A. 1989, ApJS, 69, 703
Savage, B. D., & Mathis, J. S. 1979, ARA&A, 17, 73
Tytler, D., & Fan, X.-M. 1992, ApJS, 79, 1
Ward, M., Elvis, M., Fabbiano, G., Carleton, N. P., Willner, S. P., & Lawrence, A. 1987, ApJ, 315, 74
Wilkes, B. J., & Elvis, M. 1987, ApJ, 323, 243
Williams, O. R., et al. 1992, ApJ, 389, 157
Wills, B. J., Netzer, H., & Wills, D. 1985, ApJ, 288, 94